SAND2013-6580C

Design of Wearable Binoculars with On-Demand Zoom

Robert R. Boye, Ronald S. Goeke, Jeffery P. Hunt, Aaron M. Ison, Bradley H. Jared, Jamin R. Pillars, Michael P. Saavedra, William C. Sweatt, W. Graham Yelton, Edward G. Winrow, Steve L. Wolfley

Sandia National Laboratories
PO Box 5800
MS 1082
Albuquerque, NM 87185

ABSTRACT

Sandia has developed an optical design for wearable binoculars utilizing freeform surfaces and switchable mirrors. The goals of the effort included a design lightweight enough to be worn by the user while providing a useful field of view and magnification as well as non-mechanical switching between normal and zoomed vision. Sandia's approach is a four mirror, off-axis system taking advantage of the weight savings and chromatic performance of a reflective system. The system incorporates an electrochromic mirror on the final surface before the eye allowing the user to switch between viewing modes. Results from a prototype of a monocular version with 6.6x magnification will be presented. The individual mirrors, including three off-axis aspheres and one true freeform, were fabricated using a diamond-turning based process. A slow-slide servo process was used for the freeform element. Surface roughness and form measurement of the freeform mirror will be presented as well as the expected impact on performance. The alignment and assembly procedure will be reviewed as well as the measured optical performance of the prototype. In parallel to the optical design work, development of an electrochromic mirror has provided a working device with faster switching than current state of the art. Switchable absorbers have been demonstrated with switching times less than 0.5 seconds. The deposition process and characterization of these devices will be presented. Finally, details of an updated optical design with additional freeform surfaces will be presented as well as plans for integrating the electrochromic mirror into the system.

Keywords: Freeform optics, Head-mounted optics, Diamond-turning, Reflective optics, Electrochromic, Switchable mirror

INTRODUCTION

Sandia has developed an optical design for wearable binoculars utilizing freeform surfaces and prototyped the first iteration of the optical design as well as a switchable mirror for eventual integration in the system. The goals of the effort include a design lightweight enough to be worn while providing a useful field of view and magnification as well as a method for switching between normal and zoomed vision. We have chosen to pursue a reflective design to leverage some of the inherent advantages of mirrors including freedom of material choice, absence of chromatic aberrations and the compact telephoto advantage of a folded geometry.[1] Of course, the tradeoffs of a reflective system must also be acknowledged. Since the system will be a binocular, the optical elements will necessarily be off-axis segments. Further, reflective systems often have a small field of view (FOV) as well as a higher sensitivity to the surface figure of the optical elements.

To address the size of the FOV, we examined the applicability of three-mirror anastigmat (TMA) designs.[2] Centered systems of three mirrors with power can correct for spherical aberration as well as coma and astigmatism. Additionally, the proper choice of power distribution among the elements can eliminate field curvature and leads to classical TMA designs with two concave (positive) mirrors before and after a convex (negative) element. This ability for increased aberration correction as compared to simpler one- and two-mirror designs enables these systems to function over an increased FOV.

The eventual prototype design provided magnification of M=6.6x, a FOV of 4.5º, and very good image quality. Implementation of a prototype monocular required the fabrication of the mirrors including three off-axis aspheres and one true freeform. They were fabricated using diamond-turning with a slow-slide servo approach used for the freeform element. Surface roughness of the fabricated mirrors was less than 10 nm Sa without post-polishing and form measurement of the freeform mirror was less than 0.5 μm across the majority of the aperture. The alignment and assembly of the system was done using a combination of passive (visual) and active alignment. The results from the prototype led to the development of advanced designs using additional freeform surfaces to further extend the performance of the system to rival refractive based designs.

In parallel to the development of the optics, development of an electrochromic mirror has been done to provide a means for switching the final mirror (the one directly before the eye) between reflection and transmission. Electrochromic devices have the property of changing light transmission in response to an applied voltage as ions and charge balancing electrons are intercalated into the electrochromic film in the device. Electrochromic devices based on tungsten oxide, WO_3, have been ideal for use in devices optimizing thermal control and improving energy efficiency such as "switchable" or "smart" windows.[3] These devices are inherently low power since they typically only draw significant current while switching states. Additionally, electrochromic materials can be deposited conformally on non-planar surfaces allowing their direct application to the optics system with a negligible increase in mass. Electrochromism is also instrumental in optical systems where electrochromic films can be used as selective absorbers for a particular range of wavelengths in the electromagnetic spectrum or alternatively, ranges of intensities.[4,5] To be used effectively in a visual system, the film must be capable of optically switching within the time constraint of the human eye. The human eye blinks at an approximate rate of ~400 milliseconds and the human response to an external signal is even faster, c.a. 200 milliseconds.[6] Prior to this work, WO_3 based electrochromic films have not been capable of optically switching in a sub-second time interval. We have fabricated switchable absorbers with demonstrated bleaching times less than 200 milliseconds and contrast ratios approaching 10:1. Extending the device design from the demonstrated switchable absorber to a switchable mirror has also been demonstrated; however, its optical performance still needs to be optimized.

The following section will review the evolution of the four mirror design from a conic based design to one using only aspheric surfaces to the eventual inclusion of a freeform surface. The next section will cover the mirror fabrication including results from process development on test pieces to the final prototype mirrors and their measured surface roughness and form error. The opto-mechanics, i.e. alignment and assembly, of the prototype will be reviewed as well as the prototype performance in the subsequent section of the paper. Details of the electrochromic mirror are then provided. Finally, updated design results will be shown.

OPTICAL DESIGN

A cursory examination of TMA designs uncovers the need for an additional fourth mirror to properly orient the look direction of the optics in the same direction as the user's natural gaze. This leads to the basic approach we have pursued: an off-axis, four-mirror, afocal, wide FOV design. This very description led to a possible design starting point, as shown in Figure 1.[7] This preliminary optical-system design delivers a FOV up to 10° and a magnification of 3.5× in an off-axis configuration. The design effort needed to accomplish several improvements upon this design including an increase in magnification, reduced distortion, an upright image, and increased eye relief.

Initially, this design was updated with the simple conic surfaces changed to aspheric surfaces. As the design developed, three of the four mirrors remained as rotationally symmetric aspheres with decentered pupils. Ultimately we chose to use odd aspheric surfaces described by an on-axis radius, a conic constant, and three more terms that vary as r^3, r^4, and r^5 respectively. Adding three extra terms to the basic conical surface provided enough degrees of freedom to allow a good design to be reached. In addition, the wavefront variation between the specified field points is quite smooth.

The entrance mirror (fourth from the eye) needed to have more degrees of freedom than the other three mirrors to allow the wavefront error to be corrected in both the radial and sagittal directions. The y and z position of the mirror were allowed to float, along with the tilt about the x axis, where the plane of symmetry is the yz plane. We used nine terms symmetric around the plane of symmetry up to fifth order including x^2, y^2, xy^2, y^3, x^4, x^2y^2, y^4, x^2y^3, and y^5.

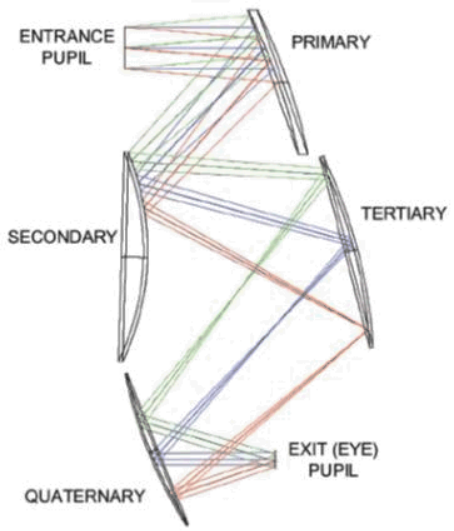

Figure 1. An off-axis, four-mirror design. This design delivers a magnifying power of 3.5× over a 10º FOV. Adapted from [7].

The image quality was corrected at ten field points on one side of the plane of symmetry. The large number of points was required because the system is considerably off axis so the image defects vary rapidly across the field. We minimized the spot sizes early in the design process and then switched to wavefront minimization as we approached a good solution. Figure 2 shows the raytrace for the design that was subsequently prototyped. The RMS wavefront error of this optical design is less than $OPD_{RMS} < 0.06\lambda$, implying that the system is diffraction-limited. The entrance pupil was chosen to be D_{EP}=6 mm to allow use under twilight conditions and to allow daytime users some tolerance between their eye position and the telescope. It was necessary to force a uniform mapping of field points in the image plane and also at the entrance mirror. In the prototype design, distortion was minimized as much as possible with the single freeform surface. As will be discussed later, additional freeform surfaces help to reduce distortion further. This prototype design was limited to a single freeform surface so that the fabrication process for the mirror could be proven and the alignment sensitivities could be better understood. The horizontal sag at the left and right margins is approximately 5% of the image radius; a significant improvement over the starting point design's distortion.

MIRROR FABRICATION

The freeform mirror is described by a polynomial series in X and Y such that the best fabrication method is direct machining via slow tool servoing where the desired surface geometry is generated by synchronizing linear tool position (X, Y, Z) with spindle position (theta). The fabrication and metrology of freeform surfaces involves complex processes with numerous inputs and potential error sources. Therefore to validate our slow tool servo machining, standard axis-symmetric surface geometries were fabricated in a nonstandard, non-rotationally symmetric form in order to generate and demonstrate fabrication and metrology processes for more arbitrary freeform geometries. Prior research in fast tool servo [8] and slow tool servo [9,10] equipment development have relied on tilted flats and off-axis parabolas since they facilitate the machining of non-rotationally symmetric surfaces that can be oriented to leverage on-axis metrology techniques. Similar process development work was done here at Sandia.

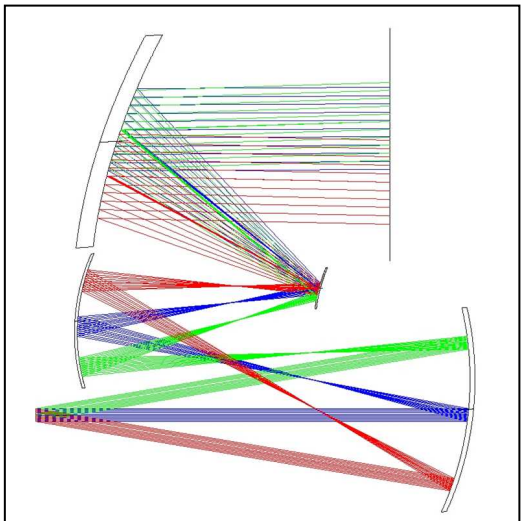

Figure 2. Raytrace of optical design used for prototype.

Process work to validate our slow tool servo fabrication strategy began with a tilted flat as it was the simplest geometry to program, to fabricate via slow tool servoing and to measure in a standard manner via on-axis form interferometry. The initial concern raised in process evaluation was whether the cutting speeds required for slow tool servoing would generate surface finishes that met system requirements. Since slow tool servoing requires coordinated motion of the z-axis with the x-axis and the work spindle, cutting velocities decrease with increases in the asymmetric departure and can therefore be more than an order of magnitude lower than that utilized in traditional turning operations. Subsequently, questions were raised regarding the potential for degradations in the material removal process (ex. tearing or burr formation), in the behavior of the cut material (ex. chip buildup or scratching) or in the rate of tool wear. For comparison with traditional machining parameters, the tilted flat was compared to a face cut flat.

While the cutting velocity for the tilted flat varied with both x-axis and spindle position, its maximum spindle speed was on the order of 170 rpm while a face cut flat was finish machined at 2000 rpm. Additional processing parameters for this

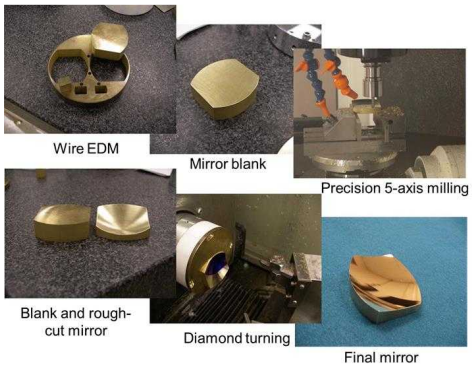

Figure 3. Process summary for mirror fabrication.

development have been reported previously. [11] Unexpectedly, the measured 0.271 µm form error of the tilted flat was about half of the 0.473 µm form error of the face cut flat. While the error for the face cut flat was not examined in great detail, its most likely source is believed to be deformation due to vacuum mounting. No degradation was observed during slow tool servoing as the surface finish for the face cut flat was generally rougher than that of the tilted flat, except at part center where both cutting processes produce a cutting velocity that approaches zero. Both flats exhibited roughness values, however, near or below 10 nm Sa.

After examining the machining of the tilted flat, an off-axis parabola was fabricated to examine a surface that more closely represented the desired freeform geometry. While a parabolic section can be cut in a rotationally symmetric manner, this part was defined in an off-axis frame, rotated about its center surface normal. Measurement and testing of the resulting parabolic mirror are straightforward since a parabola is well understood both geometrically and optically. The surface form error obtained on a Zeiss F-25 micro-CMM was 0.96 µm (peak-to-valley). While the form error did increase over both the tilted flat and the face cut flat, it remains within the requirements for the optical system. As with the tilted flat, the finish across the part radius remains at or below the 5 nm Sa.

With the diamond turning process for the optical surface validated, the mechanical requirements for the mirrors of the prototype necessitated further process development. The mirrors were off-axis sections of aspheric or freeform surfaces so mirror blanks with the proper exterior dimensions had to first be cut from blanks using micro wire-EDM. The large sags required for some of the mirrors resulted in a significant amount of material needing to be removed from the blank. To save time and tool wear while removing this material, a micro-milling step was added before the diamond machining process. This required the development of custom alignment fixtures to transfer the part from the 5-axis micro-milling center to the diamond turning machine. Figure 3 shows one of the mirrors at each step of the final process. Metrology on the freeform mirror is shown in Figure 4 with form error near the edges of the aperture reaching 1.8 µm (though significantly less over a majority of the aperture). Surface roughness was measured to be less than 10 nm across the part.

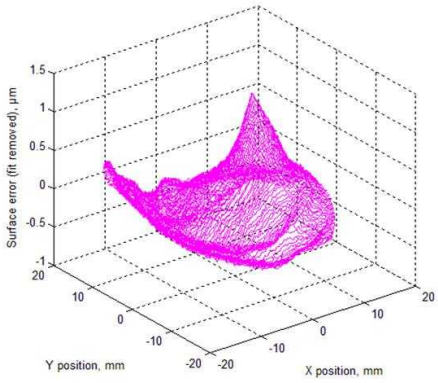

Figure 4. Form error of freeform mirror for prototype.

OPTO-MECHANICAL ALIGNMENT AND PROTOTYPE PERFORMANCE

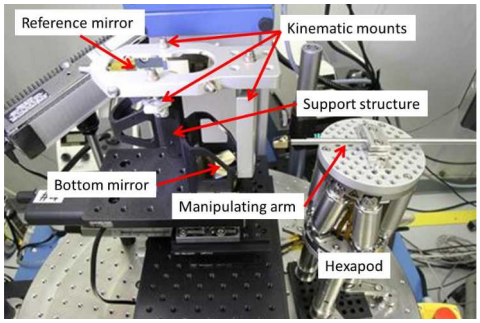

Figure 5. Alignment station for aspheric mirrors with first mirror mounted and second mirror ready to be inserted into assembly.

While the optical design was finalized, the mechanical support structure was designed as well as the alignment and assembly process. The support structure for the initial prototype had to properly support the brass mirrors while also facilitating their alignment. Since the mass of the prototype was not a concern, the material choice of aluminum was made for ease of machining. The support structure was mounted in a Trioptics™ air-bearing and focusing autocollimator system with a reference mirror attached via temporary kinematic mounts, see Figure 5. Fiducials on the reference mirror provided lateral alignment references and the autocollimator removed tip and tilt. This arrangement was used to align and mount the three off-axis mirrors. Further details of the assembly process have been previously reported. [12]

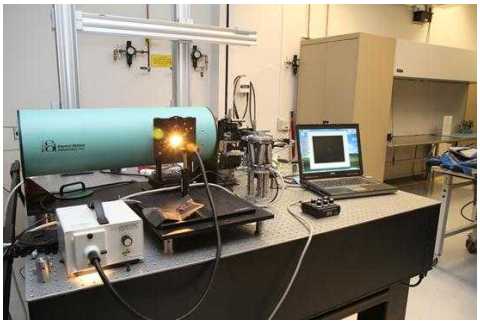

Figure 6. Active alignment station for freeform mirror placement.

The final mirror to be aligned was the freeform element. An initial alignment sensitivity analysis indicated that the alignment tolerances for this element were fairly large, e.g. 50 μm or more for lateral alignment, but it was decided to do an active alignment of this element to insure the best alignment could be achieved repeatably. A collimator and point source microscope were setup to actively measure the output of the design while the final mirror was aligned. The point source microscope was used with its objective removed to test the collimated output of the full prototype. The operator could manipulate the mirror while minimizing the focused spot produced by the optical assembly, see Figure 6. Care was taken to initially align the collimator and point source microscope, but the alignment of the final mirror was found to be straightforward and repeatable.

The full prototype assembly is shown in Figure 7 with and without the outer cover. The output of the point source microscope used during alignment provided an experimental point spread function (PSF) for the assembly. There was noticeable power outside the central spot as shown in Figure 8. The metrology data taken on the freeform mirror, Figure 4, was added to the original model of the design. This resulted in a simulated PSF that qualitatively matched the performance seen in the assembly and identified form error as the major contributor to the PSF performance.

Figure 7. Full monocular prototype. Right image includes cover used to eliminate stray light during viewing.

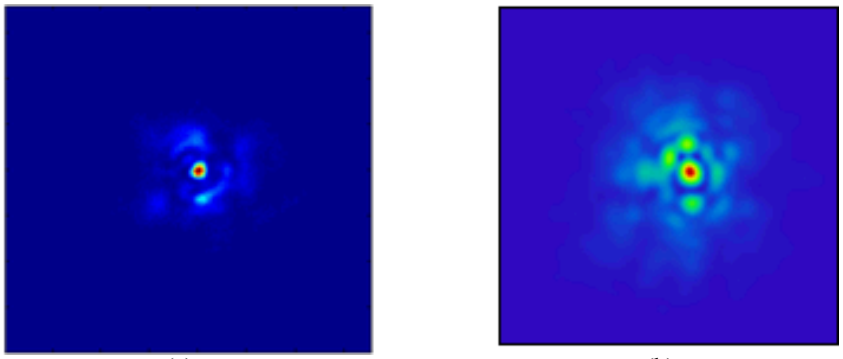

(a) (b)

Figure 8. Measured PSF of prototype (a) and simulated PSF (b) using metrology data of form error of freeform element. The observed asymmetry of the prototype is well reproduced by adding the measured form error of the freeform mirror to the design.

Analysis of resolution chart images resulted in the MTF response shown in Figure 9. The transform of the PSF image is also included. While the MTF performance is reduced from the ideal design values, the performance still provides excellent imagery for a visual system. Note that the resolution of the eye is often stated as having a cutoff of 30 cycles per degree and the prototype provided good response at this spatial frequency. A qualitative image is shown in Figure 10

and shows that the image quality compares well with a high quality digital camera image. The color is due to the prototype's uncoated brass mirrors.

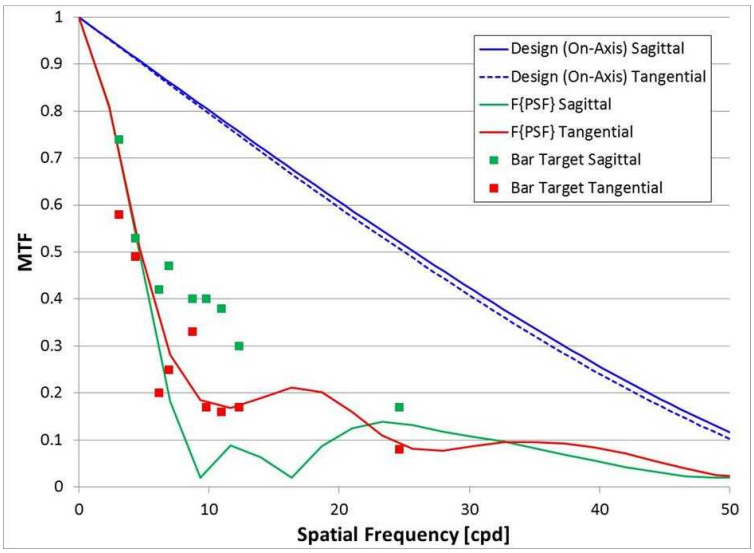

Figure 9. MTF of prototype determined from resolution chart images (points) and PSF transform (lines).

Figure 10. Images taken with a high quality digital SLR (zoomed appropriately, left) and through the prototype with an unzoomed camera (right). Note that the color in the prototype image is due to the brass mirrors being uncoated.

ELECTROCHROMIC MIRROR DEVELOPMENT

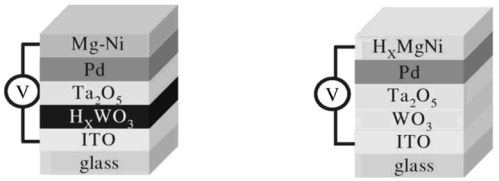

Figure 11. Thin film stack of electrochromic mirrors in reflective (left) and transmissive state (right) (from [13]).

The design of the electrochromic mirror is based on a stacked thin film device as shown in Figure 11, following work done by Tajima and coworkers. [13] The Mg-Ni layer is the material that switches between reflective and transmissive states. The Pd layer acts as a proton injector and diffusion barrier. The final device also has a thin Al layer underneath the Pd to also act as a diffusion barrier. [14] The tantalum oxide, Ta_2O_5, is the solid electrolyte. The WO_3 switches between absorbtive and transmissive states and the ITO layer is the bottom conductor for the device. As shown in Figure 11, when protons are present in the WO_3 layer, it is absorptive and the Mg-Ni layer is reflective. By applying a voltage the protons can be moved from the WO_3 layer to the Mg-Ni making both layers transmissive. The development of the switchable mirror was done in stages with the preliminary work done on the absorbing half of the device.

To increase the optical switching speed, the atomic arrangement of the films must be controlled. A hexagonal structure is favored as it forms a porous structure with open spaces for ion intercalation between the WO_6 octahedra that make up the WO_3 film.[15] Deposition parameters during reactive sputtering such as power, O_2 and Ar flow rates, and pressure, can be varied to control the porosity and thus the ion intercalation and speed of the films. The stoichiometry of the films is also controlled through these parameters and contributes to the performance of the films.[16,17]

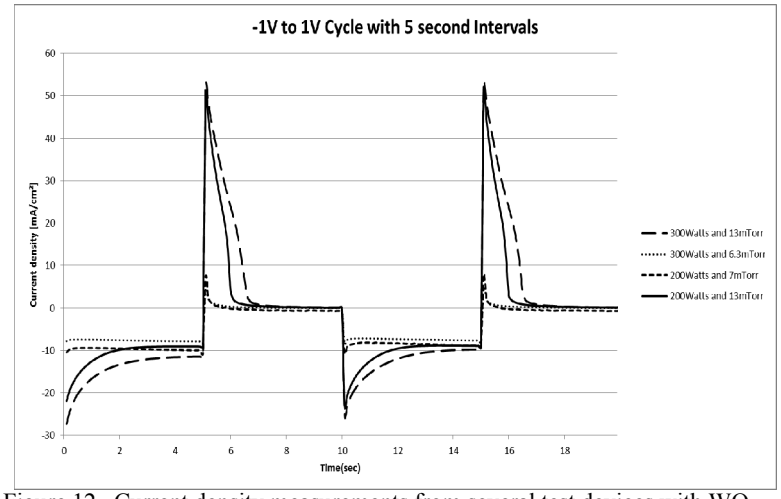

Figure 12. Current density measurements from several test devices with WO_3 deposited at differing pressures.

Indium tin oxide (ITO) coated glass slides were used as substrates for the WO_3 and Ta_2O_5 films. The films were deposited using reactive pulsed DC magnetron sputtering with pure tungsten and tantalum targets. Test runs were completed with the sputtering system to determine Ar and O_2 flow rates to achieve the proper stoichiometry for both the WO_3 and Ta_2O_5 films. The deposition pressure and the power were also varied to optimize film performance considering both speed and transmission range.

The electrolyte, Ta_2O_5, also serves as a protective layer for testing WO_3 in an acidic aqueous environment half-cell arrangement. The aqueous chemistry consisted of 1M H_2SO_4 and 10% by volume glycerol and provided protons during testing. The films were cycled by applying an alternating voltage in 1 to 5 second intervals. The current density was measured during switching and electrochemical impedance measurements on the films provided interfacial resistance measurements. Low current density peaks corresponded to small optical transmission ranges. As shown in Figure 12, higher deposition pressures provided higher current densities. Also, higher pressures led to lower interfacial resistance, see Figure 13, leading to faster switching. Optical properties of the films were also measured with an example result shown in Figure 14. This plot shows the change in transmission at 600 nm with transmission switching from 12% to 92%. The inset of the Figure shows a test device in a half-cell arrangement bleached and darkened.

It is interesting to note that films deposited with lower pressures did not perform as well. While lower pressures are preferred for more compact and durable films, electrochromic applications require a more porous and less dense film for faster switching speeds due to more space for ion intercalation.[15] The best performing films used WO_3 layers deposited with a pressure of 24.5 mTorr. Other parameters for the WO_3 deposition included an Ar flow rate of 138.9

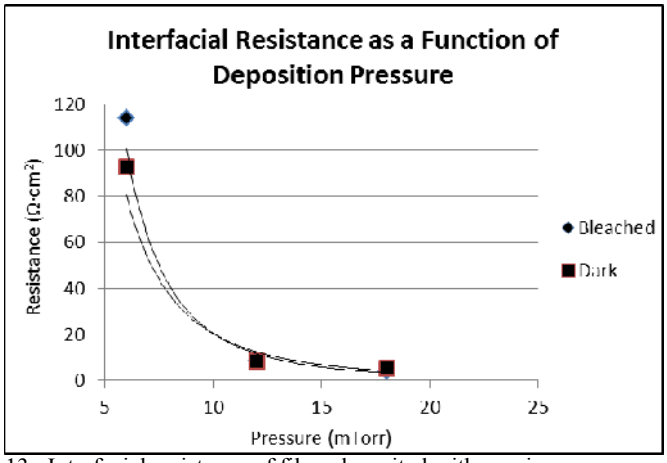

Figure 13. Interfacial resistance of films deposited with varying pressures. Note, data points for bleached films at 12 and 18 mTorr are obscured by data for darkened films.

sccm, O_2 flow rate of 21.3 sccm and power of 200 W. The parameters for the Ta_2O_5 deposition were a pressure of 12 mTorr, Ar flow of 55.5 sccm, O_2 flow of 13.9 sccm, and power of 300W. The optimal thicknesses for the WO_3 and Ta_2O_5 layers were 150 and 100 nm, respectively.

Once the optimal parameters for the absorbing half of the switchable mirror were determined, the development of the Mg-Ni layer began. The deposition of the Mg-Ni alloy requires a co-deposition of two materials with vastly different partial pressures. The optimization of the Mg-Ni portion of the device was hampered by the practicalities of the half-cell testing. The acidic electrolyte used with the tungsten oxide samples quickly destroyed the Mg-Ni samples. Use of a base solution (0.1M KOH), allowed for testing the parts, but the low concentration of H^+ led to slow switching measurements. Despite this difficulty, a switching time less than 6 seconds (3 seconds for the bleaching cycle) was achieved by

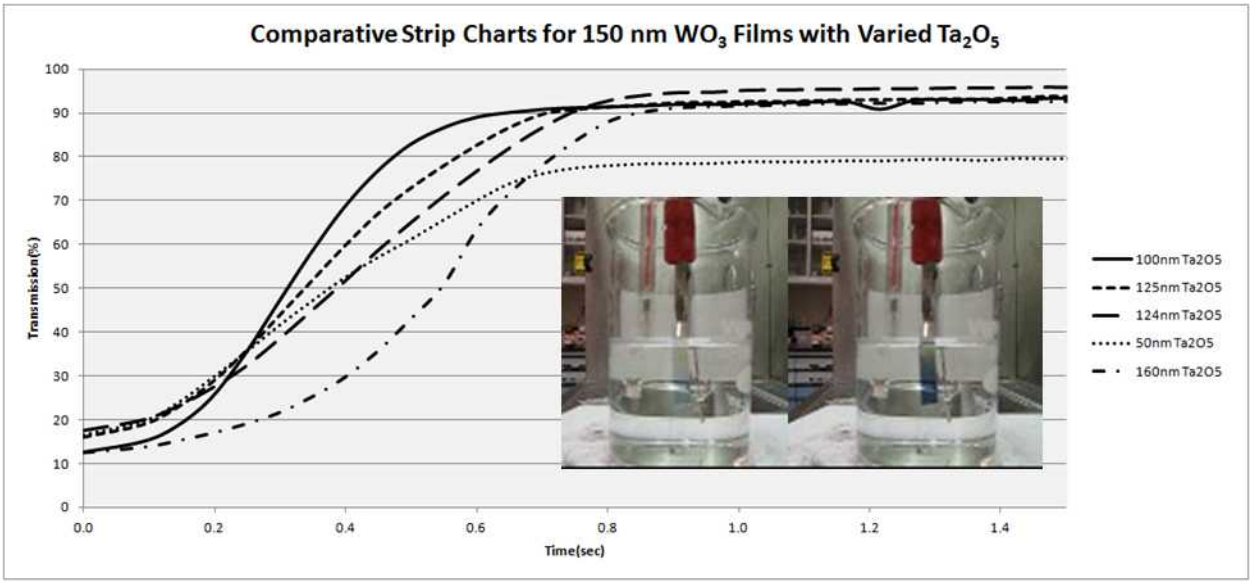

Figure 14. Switching transmission of test devices.

changing the stoichiometric ratio of magnesium and nickel as well as the deposition pressure (film porosity). Tests were done with protective coatings applied to the Mg-Ni layer (Nafion and Ta_2O_5) and samples with sub-second switching were demonstrated; however, the overcoats did not provide much protection and these samples only survived for a small number of switching cycles.

It was decided that further work with the Mg-Ni in isolation would not be effective due to the difficulties with the half-cell test arrangement. Figure 15 shows pictures of a device in the reflective and transmissive states. The low transmission is due, in part, to the ratio of magnesium and nickel. Further optimization work will look at increasing the magnesium content to allow for higher transmission. The full cells were fabricated as follows:

- ITO coated substrates were purchased from an outside vendor
- WO_3 and Ta_2O_5 were deposited using parameters described earlier

- Films were protonated using sulfuric acid/glycerol chemistry
- Pd was then deposited
- Mg-Ni deposited with varying stoichiometric ratio and chamber pressure

Notice that the dielectric portion of the device was protonated using essentially the same half-cell arrangement used for testing. This is a crucial step that injects the device with a supply of hydrogen ions required for operation. Figure 15 shows the switching times for one of the fabricated devices. It is important to note that the device design can have a significant effect on the switching time of the device. Contact geometry and different current density for the two sides of the device can be tailored to improve performance. The switching times shown in Figure 15 were achieved without using patterned gold on either side of the device or an asymmetric power output.

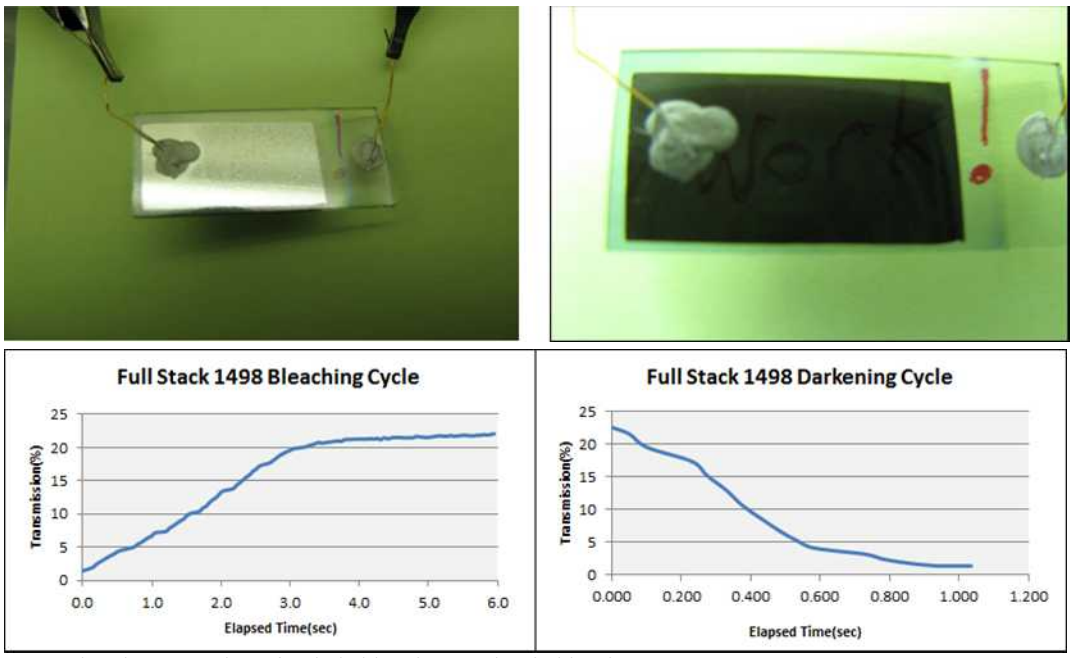

Figure 15. First demonstration of switchable mirror and switchingtimes.

ADVANCED OPTICAL DESIGN PROGRESS

The successful freeform mirror fabrication and monocular prototype development motivated the design of an advanced telescope system with improved optical performance. The improvements were possible because the three aspheric surfaces were re-defined as freeforms. The additional degrees of freedom led to increased magnification of M=8x with an entrance pupil of 5mm, and a field of view of FOV=3.5^0. The optical layout is presented in Figure 16. This design has much less distortion than the previous design; 1.2% radially and ±0.6% in the radial direction, and it has diffraction-limited imagery over a circular image plane. Additionally the eye clearance has been increased dramatically (compare Figures 2 and 16) from approximately 10 to 40 mm.

The updated design also assumed a plastic material for the mirror substrates to provide a dramatic reduction in mass over the brass mirror-based prototype. Simply substituting Zeonex E48R for the brass used in the prototype, the mass of the prototype could be reduced from 325 grams to 119 grams. Inspection of the mirrors in the prototype show that excess material was not removed and would allow for further mass reductions. Approximate estimates for an updated monocular mass are 50 grams.

Utilizing plastic for the mirror substrates requires updated machining processes and the first iteration of devices has been done, see Figure 17. The mirror substrate has been cut on both sides to minimize mass, but notice that the order of process has been changed to accommodate this two sided part. Previously, the exterior dimensions of the brass mirrors

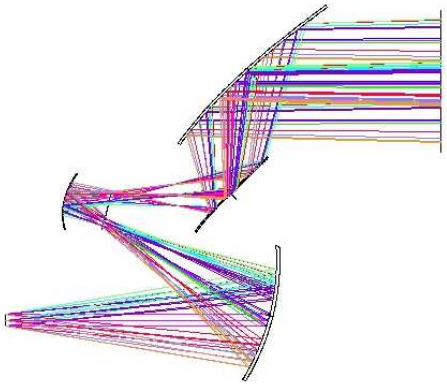

Figure. 16: Next generation all-reflective M=8X telescope with low distortion

were cut to form the original blank. For this process, the starting material was machined around the edge to provide mechanical fixturing elements while the optical surfaces were machined. After the optical surfaces are defined, the mirror's exterior dimensions will be cut out.

CONCLUSIONS

Sandia has developed an optical design and prototyped "wearable binoculars" utilizing off-axis aspheric and freeform surfaces. The design provides an adequate field of view, FOV=4.7^0, and a magnification of M=6.6X. This off-axis system provides excellent imagery, but the basic design has a moderate amount (~5%) of distortion. The first prototype of this all-reflective telescope was realized with mirrors fabricated using slow-slide servoing on a diamond-turning machine. The nano-roughness of the diamond-turning was acceptable for visual optics without a need for post-polishing. The surface form error of the freeform mirror resulted in some reduction in performance; however, the visual quality was still excellent. This effort included the successful design, fabrication, testing and assembly of an optical design based on freeform surfaces.

Subsequent design and development work extended the optical performance to M=8x with significantly reduced distortion (1.6% vs 5%) by allowing the use of freeform surfaces for each of the mirrors. Updated mirror fabrication work has also demonstrated that the design can be realized with a minimized mass allowing it to be worn by a user.

Parallel development of a switchable electrochromic mirror demonstrated sub-second switching on test devices. Partial, absorptive, devices switched as fast as 150 milliseconds (bleaching) and a transmission range as large as 12-92% was achieved. Complete switching mirrors were also demonstrated; however, the reflective layer was not optimized nor was the overall device design. Despite this, sub-second switching was demonstrated in isolated tests for the reflective half of the device and further optimization can realize a stand-alone device working with sub-second switching times.

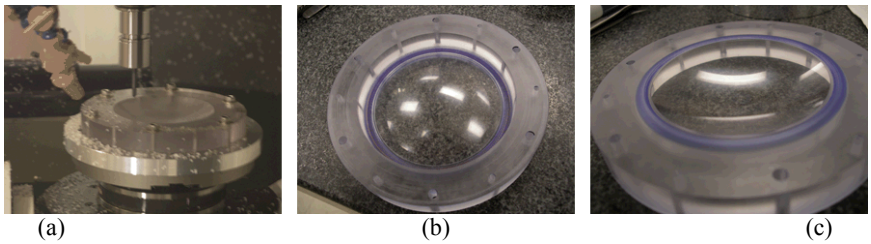

(a) (b) (c)

Figure 17. Plastic optical blank being rough-cut on 5-axis milling machine (a) and views of the convex (b) and concave (c) sides of the machined two-sided optic

ACKNOWLEDGMENT

This work was supported by the DARPA SCENICC program. Sandia National Laboratories is a multi-program laboratory managed and operated by Sandia Corporation, a wholly owned subsidiary of Lockheed Martin Corporation, for the U.S. Department of Energy's National Nuclear Security Administration under contract DE-AC04-94AL85000.

REFERENCES

1. Rudolf Kingslake, ***Lens Design Fundamentals***, Academic Press, San Diego, **1978**.
2. R.N. Wilson, ***Reflecting Telescope Optics I, 2nd ed***., Springer-Verlag, Berlin, **2007**.

3. Baetens, R.; Jelle, B. P.; Gustavsen, A., "Properties, requirements and possibilities of smart windows for dynamic daylight and solar energy control in buildings: A state-of-the-art review," *Sol Energ Mat Sol C* **2010,** *94* (2), 87-105.
4. Beni, G.; Schiavone, L. M., "Matrix-Addressable Electrochromic Display Cell," *Appl Phys Lett* **1981,** *38* (8), 593-595.
5. Weng, W.; Weng, T.; Higuchi, M.; Suzuki, T.; Fukuoka, T.; Shimomura, M.; Ono, L.; Radhakrishnan, H.; Wang, N.; Suzuki, H.; Oveisi, Y., "A High-Speed Passive-Matrix Electrochromic Display Using a Mesoporous TiO2 Electrode with Vertical Porosity," *Angewandte Chemie (International ed.)* **2010,** *49* (23), 3956-3959.
6. Volkmann, F. C.; Riggs, L. A.; Moore, R. K., "Eyeblinks and Visual Suppression," *Science* **1980,** *207* (4433), 900-902.
7. Reynold S. Kebo, US Patent No. 4,804,258 (14-February-1989).
8. Cuttino JF, Miller AC, Schinstock DE, "Performance Optimization of a Fast Tool Servo for Single-Point Diamond Turning Machines," IEEE/ASME Transactions on Mechatronics. **1999**; *4(2)*, 169-179.
9. Gubbels GP, Venrooy BW, Henselmans R., "Accuracy of freeform manufacturing processes," Proceedings of Optical Manufacturing and Testing VIII; **2009**.
10. Yin ZQ, Dai YF, Li SY, Guan CL, Tie GP, "Fabrication of off-axis aspheric surfaces using a slow tool servo," International Journal of Machine Tools and Manufacture, **2011**, *51(5)*, 404–410.
11. Bradley H. Jared, Michael P. Saavedra, William C. Sweatt, Robert R. Boye, "Developing Capabilities for Fabricating Extended Polynomial Freeform Mirrors", Proceedings of the 27th Annual Meeting of ASPE, October 2011, San Diego, CA.
12. Robert R. Boye, William C. Sweatt, Bradley H. Jared, Aaron M. Ison, Edward G. Winrow, Michael P. Saavedra, and Jeffery P. Hunt, "Design of Head-Mounted Binoculars Utilizing Freeform Surfaces," submitted to *Optical Engineering*.
13. Kazuki Tajima, Yasusei Yamada, Shanhu Bao, Masahisa Okada, and Kazuki Yoshimura, "Durability of All-Solid-State Switchable Mirror Based on Magnesium-Nickel Thin Film," Electrochemical and Solid-State Letters, **2007,** *10(3)*, J52-J54.
14. Kazuki Tajima, Yasusei Yamada, Shanhu Bao, Masahisa Okada, and Kazuki Yoshimura, "Aluminum buffer layer for high durability of all-solid-state switchable mirror based on magnesium-nickel thin film," Applied Physics Letters, 2007, *91(5)*, 051908-1 – 051908-3.
15. Granqvist, C. G., "Oxide electrochromics: An introduction to devices and materials," *Sol Energ Mat Sol C* **2012,** *99*, 1-13.
16. Sato, R.; Kawamura, N.; Tokumaru, H., "The coloration of tungsten-oxide film by oxygen deficiency and its mechanism," *Appl Surf Sci* **2008,** *254* (23), 7676-7678.
17. Georg, A.; Graf, W.; Wittwer, V., "Comparison of electrical conductivity and optical properties of substoichiometrically and electrochemically coloured WOx films of different crystallinity," *Sol Energ Mat Sol C* **1998,** *51* (3-4), 353-370.